IAI
Journals.ASM.org

In Vivo-Induced InvA-Like Autotransporters Ifp and InvC of *Yersinia pseudotuberculosis* Promote Interactions with Intestinal Epithelial Cells and Contribute to Virulence

Fabio Pisano,[a] Annika Kochut,[a] Frank Uliczka,[a] Rebecca Geyer,[a] Tatjana Stolz,[a] Tanja Thiermann,[a] Manfred Rohde,[b] and Petra Dersch[a]

Abteilung Molekulare Infektionsbiologie, Helmholtz-Zentrum für Infektionsforschung, 38124 Braunschweig, Germany,[a] and Department of Medical Microbiology, Helmholtz-Zentrum für Infektionsforschung, 38124 Braunschweig, Germany[b]

The *Yersinia pseudotuberculosis* Ifp and InvC molecules are putative autotransporter proteins with a high homology to the invasin (InvA) protein. To characterize the function of these surface proteins, we expressed both factors in *Escherichia coli* K-12 and demonstrated the attachment of Ifp- and InvC-expressing bacteria to human-, mouse-, and pig-derived intestinal epithelial cells. Ifp also was found to mediate microcolony formation and internalization into polarized human enterocytes. The *ifp* and *invC* genes were not expressed under *in vitro* conditions but were found to be induced in the Peyer's patches of the mouse intestinal tract. In a murine coinfection model, the colonization of the Peyer's patches and the mesenteric lymph nodes of mice by the *ifp*-deficient strain was significantly reduced, and considerably fewer bacteria reached liver and spleen. The absence of InvC did not have a severe influence on bacterial colonization in the murine infection model, and it resulted in only a slightly reduced number of *invC* mutants in the Peyer's patches. The analysis of the host immune response demonstrated that the presence of Ifp and InvC reduced the recruitment of professional phagocytes, especially neutrophils, in the Peyer's patches. These findings support a role for the adhesins in modulating host-pathogen interactions that are important for immune defense.

Enteric pathogens, including *Yersinia pseudotuberculosis*, possess a variety of multifunctional adhesins on their surface that mediate tight adhesion to mammalian cells and facilitate the successful colonization of host tissues. Some of these pathogenicity factors enable binding to different cell types and also can promote the efficient internalization of the bacteria following the initial cell adhesion process (38, 47). Invasion can protect the bacteria against host immune responses, allowing them to penetrate epithelial cell layers and disseminate into deeper tissues. Genome analysis further revealed that several bacterial pathogens encode more than 10 different surface adhesins which could be important during different stages of the infection (10, 40, 45, 59). Alternatively, they may contribute to the tissue and/or host tropism of the microbes.

Y. pseudotuberculosis is a Gram-negative zoonotic pathogen that causes several diseases, including enteritis, diarrhea, lymphadenitis, and autoimmune disorders (9). It encodes two of the best-characterized non-pilus-associated adhesins, invasin (InvA) and YadA, that are anchored to the outer membrane. Both adhesion factors promote binding and uptake by M cells and allow the efficient colonization of Peyer's patches (PP), mesenteric lymph nodes (MLN), liver, and spleen.

InvA was shown to be the most efficient invasion factor in promoting the tight binding and uptake of the bacteria into host cells (29). Translocation through the gut epithelium during the initial stages of the infection is mediated primarily by InvA, which promotes strong binding to different members of the β_1-integrin receptor family that is expressed on the apical surface of M cells (39, 48). Invasin is part of a large adhesin family of enteropathogenic bacteria that includes the intimins of enterohemorrhagic and enteropathogenic *Escherichia coli* (EPEC and EHEC, respectively), *Citrobacter freundii*, and *Hafnia alvei*, which are implicated in attaching and effacing lesions. All members of the invasin/intimin family interact with receptors integrated into the plasma membrane of the host cell that send signals to the eukaryotic cytoskeleton and lead to the tight attachment or internalization of the pathogenic bacteria (20, 51). The most conserved region between the family members (>40% identity) encompasses the N-terminal 500 amino acids. This part of the protein is predicted to form a β-barrel structure in the outer membrane (OM), acting as an autotransporter of the surface-exposed C terminus. It is absolutely required for the secretion, assembly, and incorporation of the molecules into the OM and is necessary for the proper surface presentation of the cell adhesion domain (60). The cell binding activity of invasin and the intimins is localized within the last C-terminal amino acids. The receptor specificity and sequence of this adhesive portion varies significantly among the invasin/intimin homologues (10 to 20% identity). In the case of invasin, the surface-exposed region folds into four globular, predominantly β-stranded immunoglobulin-like domains, and the most external domain forms a C-type lectin-like super domain, which is required for cell adhesion and invasion via binding to β_1-integrins (Fig. 1) (16, 21, 27).

In the absence of InvA, the trimeric autotransporter YadA can promote adhesion and uptake (7, 17). This adhesin mediates adherence into epithelial cells and professional macrophages

Received 27 July 2011 **Returned for modification** 5 September 2011
Accepted 4 December 2011
Published ahead of print 12 December 2011
Editor: J. B. Bliska
Address correspondence to Petra Dersch, petra.dersch@helmholtz-hzi.de.
F. Pisano, A. Kochut, and F. Uliczka contributed equally to this work.
Supplemental material for this article may be found at http://iai.asm.org.

doi:10.1128/IAI.05715-11

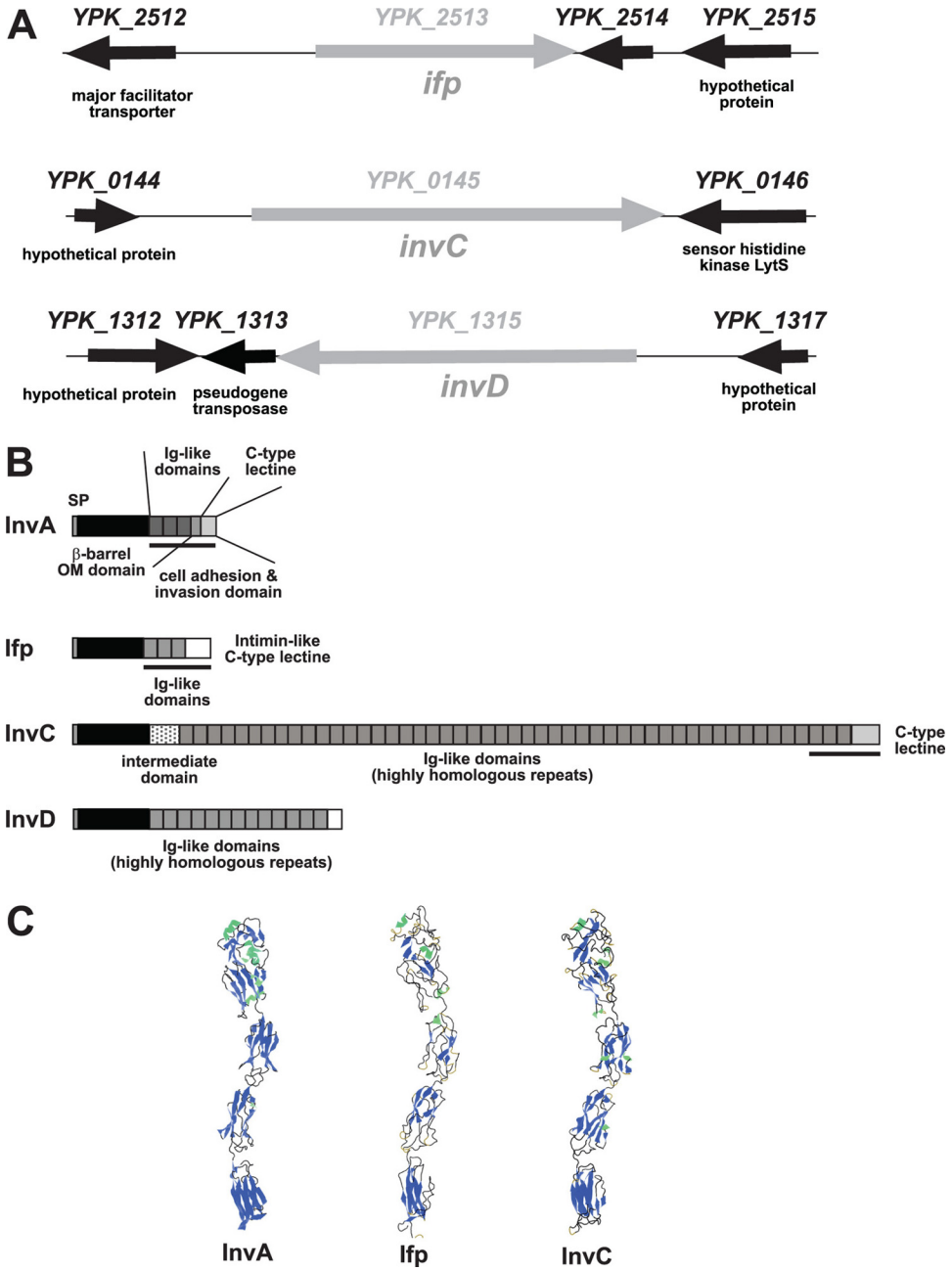

FIG 1 Overview of invasin and InvA-like proteins of *Y. pseudotuberculosis*. (A) Chromosomal loci of the *ifp*, *invC*, and *invD* gene in the genome of YPIII. (B) Scheme of the domain structures of the invasin-like autotransporter proteins of YPIII. The black bar underneath the linear protein structure indicates the portion of the external domain illustrated in panel C. (C) Structure of the external cell binding domain of invasin and predicted structures of the surface-exposed homologous Ifp and InvC proteins.

through binding to extracellular matrix (ECM) proteins, such as collagen, laminin, and fibronectin (19, 54). YadA belongs to a family of trimeric autotransporter proteins that form lollipop-shaped surface projections that densely cover the bacterial surface as a capsule-like structure (24). It consists of an outer membrane anchor domain at the C terminus, an intermediate segment forming a coiled-coil pillar-like stalk, and a bulky lock-nut N-terminal head structure (46). Evidence has been provided that different pathogenic functions are attributable to certain portions of the molecule which can vary between the highly homologous YadA proteins of different species and serotypes. The head domain is involved in autoagglutination and promotes adherence to host cells (e.g., neutrophils) and extracellular matrix proteins (19). An internal region of the *Y. pseudotuberculosis* YadA head domain also is critical for ECM-specific substrate recognition and bacterial internalization into epithelial cells, which was shown to occur through fibronectin-bound β_1-integrin receptors (23). YadA also protects *Yersinia* against the bactericidal activity of the serum complement system and defensins by binding the serum complement factors H and the C4 binding protein (5, 6, 32). Although

YadA promotes significant cell attachment and entry via β_1-integrins into eukaryotic cells similarly to InvA (17, 23), translocation assays in mice indicate a different role for YadA during intestinal colonization. YadA is induced under different environmental conditions and seems to be important for the colonization of epithelial cells rich in mucus at the PP surface (39). This may facilitate the replication of the bacteria in the mucosal surface and increases the effective dose of the pathogen at the epithelial surface. Furthermore, it was shown that in the absence of YadA and InvA other *Y. pseudotuberculosis* virulence factors can compensate for efficient translocation across the intestinal epithelium, and this pathway seems to bypass the colonization of the PPs (2, 39). During recent years two other ligands were identified that can interact with host cells, the pH6 antigen and the outer membrane protein Ail. However, *psaA* and *ail* mutants showed the same ability as the wild type to penetrate the mouse intestinal mucosa and colonize the Peyer's patches early after infection (37, 39).

An inquiry into the genome sequence of *Y. pseudotuberculosis* YPIII revealed multiple genes for additional putative adhesion factors with significant similarity to invasin, YadA, Ail, and adhesins of other pathogens. In this study, we characterized the function of two InvA-type proteins of *Y. pseudotuberculosis* YPIII, Ifp and InvC. We demonstrate that Ifp and InvC are adhesins that mediate interaction with human, murine, and porcine intestinal cells and affect the colonization of the PPs. The Ifp protein contributes to *Y. pseudotuberculosis* virulence in mice, whereas InvC does not seem to play a major role in this infection model.

MATERIALS AND METHODS

Bacterial strains, cell culture, media, and growth conditions. The strains used in this study are listed in Table 1. Overnight cultures of *E. coli* were routinely grown at 37°C, and *Yersinia* strains were grown at 25 or 37°C in LB (Luria-Bertani) broth. The antibiotics used for bacterial selection were the following: ampicillin, 100 μg/ml; chloramphenicol, 30 μg/ml; kanamycin, 50 μg/ml; and gentamicin, 50 μg/ml. No differences between the *in vitro* growth characteristics of the *Y. pseudotuberculosis* mutants and those of the wild-type strain were observed. For *in vitro* infection experiments, bacteria were grown to stationary phase, washed, and diluted in phosphate-buffered saline (PBS) to an optical density at 600 nm (OD_{600}) of approximately 1 to 2 in PBS.

Human HEp-2 cells were cultured in RPMI 1640 medium with GlutaMAX (Invitrogen) supplemented with 7.5% newborn calf serum (Sigma-Aldrich) at 37°C in the presence of 5% CO_2. Human Caco-2, murine Mode-K, and porcine IPEC-J2 cells were grown in Dulbecco's modified Eagle medium (DMEM)-Ham's F-12 (Biochrom) supplemented with 10% fetal bovine serum (FBS) Superior (Biochrom).

Computational analysis of the *ifp* and *invC* genes. The *ifp* and *invC* loci were identified in all four available whole-genome sequences of *Y. pseudotuberculosis* strains. The *invA* sequence of *Y. pseudotuberculosis* was used for alignment with the microbial genome BLAST database, which is available from the National Center for Biotechnology Information (NCBI) website (http://www.ncbi.nlm.nih.gov/sutils/genom_table.cgi). An inter- and intrastrain alignment and protein motif analyses were performed with online software of EMBL-EBI (http://www.ebi.ac.uk/Tools) and the KEGG database (http://www.genome.jp/kegg/).

DNA manipulations and cloning of the *ifp* and *invC* genes. All DNA manipulations, PCR, restriction digestions, ligations, and transformations were performed using standard techniques as described previously (38, 48). Plasmids and primers used in this study are listed in Table 1 (also see Table S1 in the supplemental material). Plasmids pFU08 (ifp_{his6}) and pFU140 (ifp^+) were constructed by the amplification of *ifp* (YPK_2513) from genomic DNA of *Y. pseudotuberculosis* YPIII with primer pairs I447/I448 and I447/I446 and integrated into the XhoI and KpnI sites, respectively, of pBAD/Myc-HisC (Invitrogen). The *invC* (YPK_0145) gene was cloned in three steps. First, two fragments harboring the 5′ and 3′ segments of the *invC* gene (positions 3 to 2745 and 12487 to 16011) were amplified with primer pairs I974/I466 and I977/I975, digested by SacI/EcoRI and EcoRI/HindIII, and ligated into the SacI and HindIII sites, respectively of pBAD/Myc-HisA. In the next step, plasmid pFU40 was constructed to harbor the internal fragment of the *invC* gene, including bp 2469 to 16011. Chromosomal DNA of *Y. pseudotuberculosis* YPIII was extracted with Qiagen Genomic-tip 100/G columns and digested with AatII and EcoRI. The resulting chromosomal fragments of ~10 kb, including a 10,068-bp fragment containing the internal repetitive sequences of *invC*, were separated by gel electrophoresis, extracted on a blue light transilluminator by using Gel Star nucleic acid gel stain (Biozym), and ligated into AatII and EcoRI sites of pZS*24MCS. The resulting colonies were screened by colony hybridization as described previously (52) using a digoxigenin-labeled *invC* probe (primers I481 and I482). The resulting plasmid pFU40 was digested with AatII and EcoRI and ligated into AatII and EcoRI of pFU39, generating pFU41 (*invC*-his_6). Plasmid pFU141 ($invC^+$; without the His_6 tag) was constructed by the insertion of a PCR fragment amplified with primers I977 and II395 into the EcoRI and HindIII sites of pFU41. Plasmids pFU209 and pFU210 were derived from pFU41 and pFU141 by the insertion of a PCR fragment amplified with primers II631 and I466 into the SacI and AatI sites. Plasmid pFU234, containing the *ifp* upstream region and the *ifp* gene, was constructed by the insertion of a PCR fragment amplified with primers II316 and III798 from chromosomal DNA of *Y. pseudotuberculosis* YPIII into the BamHI/NotI sites of pFU109. All clones were confirmed by sequencing (GATC, Konstanz, Germany).

Construction of the *invA*, *ifp*, and *invC* reporter gene fusions. For *luxCDABE* and $gfp_{mut3.1}$ reporter gene fusions on plasmids pFU143-145 and pFU146-148, the promoter regions of *invA* (primer pair 64/II385), *ifp* (primer pair II316/II386), and *invC* (primer pair II318/II387) were amplified and ligated into the BamHI/SalI sites of pFU98 and pFU58. The exchange of the origin of replication (ori) was generated by the insertion of an AvrII/SpeI fragment of pZE12-luc into the AvrII/SpeI sites of pFU98 and pFU143-pFU145, resulting in pFU189 and pFU217-219, respectively.

The resulting plasmids were transformed into *Y. pseudotuberculosis* YPIII. Three independent cultures of the *Y. pseudotuberculosis* fusion strains were diluted to an optical density at 600 nm (OD_{600}) of 0.1, and the OD_{600} was determined subsequently to monitor growth under the indicated growth conditions (in complex and minimal media at 25 and 37°C). In parallel, bioluminescence was detected in nonpermeabilized cells with a Varioskan Flash (Thermo Scientific) using SkanIt software (Thermo Scientific). Bioluminescence was measured for 1 s every 30 min and is given in relative light units (RLU/OD_{600}) from three independent cultures performed in duplicate. *Y. pseudotuberculosis* harboring the empty vector plasmid analyzed under identical conditions had a very low detectable background level of luciferase activity; this was subtracted from the presented values.

Construction of the *ifp* and *invC* mutant strains YP97 and YP98. The mutant strains YP97 (YPIII Δ*ifp*) and YP98 (Δ*invC*) were constructed using the lambda RED recombinase system (15). For the construction of the *ifp*-deficient strain YP97, the chloramphenicol resistance gene was amplified from pKD3 with primer pair I814/I813, which contains 60 nucleotides that are homologous to the up- or downstream region of the *ifp* gene. For the *invC* mutant strain YP98, in which the first 2,671 nucleotides were replaced by a chloramphenicol resistance cassette, the *cat* gene was amplified from pKD3 with primer pair I817/I818, which has 60 nucleotides that are homologous to the upstream region and internal region downstream of nucleotide 2672 of the *invC* gene. The PCR fragments were transformed into *Y. pseudotuberculosis* YPIII pKD46 and plated on LB chloramphenicol plates. Chloramphenicol-resistant transformants were selected, and *ifp* and *invC* mutations were confirmed by PCR. Mutant strains without the plasmid pKD46 were isolated after growth in media without antibiotics.

TABLE 1 Bacterial strains, plasmids and primers

Strain or plasmid	Description	Source or reference
Bacterial strains		
E. coli K-12		
DH101β	F$^-$ *endA1 recA1 galE15 galK16 nupG rpsL* Δ*lacX74* Φ80*lacZ*ΔM15 *araD139* Δ(*ara,leu*)7697 *mcrA* Δ(*mrr-hsdRMS-mcrBC*) λ$^-$	Invitrogen
CC118λ*pir*	F$^-$ Δ(*ara-leu*)7697 Δ(*lacZ*)74 Δ(*phoA*)20 *araD139 galE galK thi rpsE rpoB arfE*^{am} *recA1*	36
Y. pseudotuberculosis		
YPIII	pIB1, wild type	8
YP9	YPIII, Δ*invA*::*tet*	39
YP97	YPIII, Δ*ifp*::*cat*	This study
YP98	YPIII, Δ*invC*(Δ1-2671)::*cat*	This study
IP32953	pIB1, wild type	10
IP32953 ΔIFP	IP32953, Δ*ifp*::*kan*	57
Plasmids		
pBAD/Myc-HisA	Cloning and expression vector	Invitrogen
pBAD/Myc-HisC	Cloning and expression vector	Invitrogen
pFU08	pBAD/Myc-HisC, ifp_{his6}^+, Ap^r	This study
pFU31	pZE12lucMCS, *egfp*	62
pFU36	pFU31, promoterless *luxCDABE*, ColEI ori, Ap^r	62
pFU39	pBAD/Myc-HisA, *invC*(Δ2746-12486), Ap^r	This study
pFU40	pZS*24MCS, *invC* (bp 2469-12546), Kn^r	This study
pFU41	pFU39, $invC_{his6}^+$, Ap^r	This study
pFU54	pFU36, promoterless *luxCDABE*, pSC101* ori, Ap^r	62
pFU58	$gfp_{mut3.1}$, Ap^r, p29807 ori	62
pFU96	*gapA-dsred2*, Ap^r, ColE1 ori	62
pFU98	pFU54, promoterless *luxCDABE*, pSC101* ori, Cm^r	62
pFU109	pSC101* ori, Kn^r	62
pFU140	pBAD/Myc-HisC, ifp^+, Ap^r	This study
pFU141	pFU41, $invC^+$, Ap^r	This study
pFU143	pFU98, *invA-luxCDABE*, Cm^r	This study
pFU144	pFU98, *ifp-luxCDABE*, Cm^r	This study
pFU145	pFU98, *invC-luxCDABE*, Cm^r	This study
pFU146	pFU58, *invA-*$gfp_{mut3.1}$, Ap^r, p29807 ori	This study
pFU147	pFU58, *ifp-*$gfp_{mut3.1}$, Ap^r, p29807 ori	This study
pFU148	pFU58, *invC-*$gfp_{mut3.1}$, Ap^r, p29807 ori	This study
pFU189	pFU98, promoterless *luxCDABE*, ColE1 ori, Cm^r	This study
pFU209	pFU41, $invC_{his6}^+$, Ap^r, optimized ribosome binding site	This study
pFU210	pFU141, $invC^+$, Ap^r, optimized ribosome binding site	This study
pFU217	pFU143, *invA-luxCDABE*, ColE1, Cm^r	This study
pFU218	pFU144, *ifp-luxCDABE*, ColE1, Cm^r	This study
pFU219	pFU145, *invC-luxCDABE*, ColE1, Cm^r	This study
pFU234	pFU109, ifp^+, pSC101* ori, Kn^r	This study
pKD3		13
pKD46		13
pRI203	pBR325, $invA^+$, Ap^r	25
pZE12lucMCS		35
pZS*24MCS		35

Expression analysis and isolation of outer membrane fractions. *E. coli* strains (DH10ß and CC118λ*pir*) and *Y. pseudotuberculosis* strain YPIII were transformed with the *ifp* or *invC* expression plasmids pFU08 and pFU41. To identify optimal expression conditions for the Ifp and InvC proteins, the transformants were cultured in LB medium to exponential phase (OD_{600} of ~0.4) or stationary phase (OD_{600} of ~4.5) at 25 or 37°C. Subsequently, P_{BAD}-driven expression was induced upon the addition of arabinose (0.01 to 2%), and Ifp_{His6} and $InvC_{His6}$ production was tested after 4 to 24 h by Western blot analysis using an antibody directed against the His tag (Qiagen). The following conditions allowed the highest Ifp and InvC production levels and were used for adhesion and invasion experiments. Bacterial cultures were grown to an OD_{600} of ~0.4 at 37°C (*E. coli*) or 25°C (*Y. pseudotuberculosis*). Subsequently, 0.02% arabinose was added, and the cultures were shifted to 25°C and grown for 4 h. *Y. pseudotuberculosis* was diluted 1:50 and grown at 25°C. The expression of Ifp and InvC was induced with 0.2% arabinose at an OD_{600} of ~0.4 for 4 h. Subsequently, the cells were harvested by centrifugation at 4°C and used for whole-cell extracts (see below) or outer membrane preparations.

The preparation of the outer membranes was performed as described previously, with some modifications (7). The bacterial pellet was resuspended in 10 ml TEM buffer (10 mM Tris-HCl, 5 mM EDTA [pH 7.8], 1 mM β-mercaptoethanol). Subsequently, bacteria were lysed by passing them three times through a French press at 103,500 kPa. The cell debris was separated by low-speed centrifugation (7,000 × *g*), and membranes were pelleted from the soluble fraction in a Sorvall OTD65B ultracentrifuge at 100,000 × *g* for 1 h. The membrane fraction was resuspended in 10

ml of SM buffer (0.5% Sarkosyl, 1 mM β-mercaptoethanol). Total membranes were incubated overnight at 4°C, and the solution subsequently was centrifuged at 100,000 × *g* for 1 h. The final outer membrane pellet was resuspended in 200 μl of sample buffer (100 mM Tris-HCl, pH 6.8, 2% SDS, 10% glycerol, 3% dithiothreitol [DTT], 0.001% bromophenol blue) and analyzed by gel electrophoresis.

Gel electrophoresis, preparation of cell extracts, and Western blotting. Bacteria were grown under various environmental conditions as described above. The optical density of the cultures was adjusted, and a 1-ml aliquot was withdrawn from each culture. The cells were collected by centrifugation and resuspended in 100 μl of NuPAGE sample buffer (Invitrogen). Electrophoresis was performed in NuPAGE Novex 3 to 8% Tris-acetate gels (Invitrogen) using an XCell SureLock minicell (Invitrogen) as described in the manufacturer's instructions. To visualize the expression of the Ifp and InvC proteins, cell extracts of bacteria expressing the His-tagged version of the adhesins were prepared and transferred onto an Immobilon membrane (Millipore). The identity and expression of the adhesins were confirmed by Western blot analysis using monoclonal antibodies against the His tag (Qiagen) and a second goat alkaline-phosphate antibody (Sigma) using 5-bromo-4-chloro-3-indoylphosphate (XP) and nitroblue tetrazolium (Boehringer Mannheim) as substrates.

Cell adhesion and invasion assay. For cell adhesion and uptake assays, 5×10^4 HEp-2, Caco-2, Mode-K, or IPEC-J2 cells were seeded and grown overnight in individual wells of 24-well cell culture plates. Cells were washed three times with PBS and incubated in binding buffer (RPMI 1640 medium supplemented with 20 mM HEPES [pH 7.0] and 0.4% bovine serum albumin [BSA]) before the addition of bacteria. Approximately 5×10^6 bacteria were added to the cells and incubated at 20°C to test for cell binding or at 37°C to test for invasion (40). One hour postinfection, the cells were washed extensively with PBS. The total number of adherent bacteria was determined by cell lysis using 0.1% Triton X-100 and plating on bacterial media. Bacterial uptake was assessed 60 min after infection as the percentage of bacteria that survived killing by gentamicin, as described previously (17). For each strain, the relative level of bacterial adhesion and uptake was determined by calculating the number of CFU relative to the total number of bacteria introduced into cells. The experiments were routinely performed in triplicate.

To obtain differentiated intestinal cells in a monolayer system, 1.5×10^5 Caco-2 cells were seeded in 6.5-mm polycarbonate transwell inserts with 3.0-μm pores (Corning) and grown for 21 days in DMEM-Ham's F12 (Biochrom) supplemented with 10% fetal calf serum (FCS) (Biochrom), 10 mM HEPES (Biochrom), and 50 μg/ml amphotericin B (Sigma-Aldrich). Cell monolayers were washed with PBS and incubated in binding buffer (DMEM-Ham's F12 medium supplemented with 20 mM HEPES [pH 7.0] and 0.4% BSA). Bacteria (2×10^8) were added to the monolayer and incubated for 3 h at 25°C to determine adherent bacteria and at 37°C to enumerate internalized bacteria. Cells with adherent bacteria were washed four times with PBS, lysed with 1% Triton X-100, and plated on solid media. The number of internalized bacteria was assessed after an additional treatment with gentamicin as described above. The percentages of adherent and internalized bacteria were calculated by determining the CFU relative to the total number of bacteria added to the monolayer. The levels of statistical significance for differences in adhesion and invasion were determined by the Student's *t* test.

Scanning electron microscopy. *E. coli* K-12 cells harboring the empty vector or the Ifp and InvC expression constructs were used to infect polarized Caco-2 cells as described above, and the samples were fixed in growth medium with 1% formaldehyde. For field emission scanning electron microscopy, glass coverslip samples were fixed with a solution containing 5% formaldehyde and 2% glutaraldehyde in cacodylate buffer (0.1 M cacodylate, 0.01 M $CaCl_2$, 0.01 M $MgCl_2$, 0.09 M sucrose, pH 6.9). Dehydration was carried out in a graded series of acetone (10, 30, 50, 70, 90, and 100%) on ice for 15 min for each step. Samples then were critical-point dried with liquid CO_2 (CPD 030; Balzers Union, Liechtenstein) and covered with a gold film by sputter coating (SCD 040; Balzers Union, Liechtenstein). For examination in a field emission scanning electron microscope (DSM 982 Gemini; Zeiss, Germany), an Everhart Thornley SE detector was used with the in-lens SE detector at a 50:50 ratio and with an acceleration voltage of 5 kV.

Mouse infection. Animal work was performed in accordance with the German regulations of the Society for Laboratory Animal Science (GV-SOLAS) and the European Health Law of the Federation of Laboratory Animal Science Associations (FELASA). The infection protocol was approved by the Niedersächsisches Landesamt für Verbraucherschutz und Lebensmittelsicherhei (animal licensing committee permission no. 33.9.42502-04-055/09). Bacteria used for oral infection were grown overnight at 25°C in LB medium, washed twice, and resuspended in PBS to an OD_{600} of 1. To assess the effect of Ifp and InvC on *Y. pseudotuberculosis* virulence, groups ($n = 10$) of 7-week-old female BALB/c mice (Janvier) were orally infected with a dose of 2×10^9 bacteria of the wild-type strain (YPIII), the isogenic *ifp* (YP97) strain, or the *invC* (YP98) mutant strain using a ball-tipped feeding needle. Body weight and the general health state of the mice were monitored every day.

In addition, groups of 7-week-old female mice were orally infected with an equal mixture of 2×10^8 bacteria of *Y. pseudotuberculosis* strains YPIII and YP97 (Δ*ifp*) or with YPIII and YP98 (Δ*invC*). At appropriate times after infection, mice were euthanized by CO_2 asphyxiation. PPs, MLNs, liver, and spleen were isolated. The ileum was rinsed with sterile PBS and incubated with 100 μg/ml gentamicin to kill bacteria on the luminal surface. After 30 min, gentamicin was removed by extensive washing with PBS three times. Subsequently, all organs were weighed and homogenized in sterile PBS at 30,000 rpm for 30 s using a Polytron PT 2100 homogenizer (Kinematica, Switzerland). Bacterial organ burden was determined by plating three independent serial dilutions of the homogenates on LB plates with and without antibiotics. The CFU were counted and are given as CFU per gram of organ/tissue. The levels of statistical significance for differences in the survival and organ burden between test groups were determined by the Mantel-Cox test and the Mann-Whitney test, respectively. The competitive index relative to wild-type strain YPIII was calculated as described previously by Monk et al. (43).

For *in vivo* imaging experiments (IVIS), 5×10^8 CFU of *Y. pseudotuberculosis* YPIII, carrying the promoter of the *invA*, *ifp*, or *invC* gene fused to the bacterial *luxCDABE* operon (pFU143, pFU144, and pFU145), was administered intraorally. At the appropriate time points, mice were anesthetized using isoflurane (Baxter) and monitored using an IVIS 200 imaging system (Calipers). Photon flux was quantified using Living Image 3.0 software (Calipers).

Histology and immunofluorescence. A group of 6- to 8-week-old female BALB/c mice ($n = 5$) was orally infected with *Y. pseudotuberculosis* strain YPIII harboring an *ifp-gfp* or *invC-gfp* fusion (pFU147 and pFU148) and a P_{gapA}::*dsRed2* expression construct (pFU228). BALB/c mice were orally infected with 2×10^8 bacteria. Three days postinfection the mice were sacrificed, and the small intestine, MLNs, liver, and spleen were isolated, embedded in Tissue-Tek OCT freezing medium (Sakura Finetek), and frozen on dry ice. Subsequently, 8- to 10-μm sections were prepared using a Zeiss cryostat Hyrax C50 and mounted on Superfrost Plus slides (Thermo Scientific). Air-dried sections were fixed for 10 min in ice-cold acetone and washed twice with 1× PBS. To visualize the nuclei of the cells in the fixed tissues, sections were stained with 4′,6-diamidino-2-phenylindole (DAPI; Sigma-Aldrich). Afterwards, slides were washed twice with 1× PBS, air dried, and mounted with 80% glycerol in 1× PBS. The localization of yersiniae in the tissues and expression of the P_{ifp}::$gfp_{mut3.1}$ or P_{invC}::$gfp_{mut3.1}$ fusion of these bacteria were visualized with a Zeiss Axiovert II fluorescence microscope.

Host immune and cytokine response. To characterize the host immune response induced upon infection with the wild-type strain YPIII and the isogenic *ifp* and *invC* mutant strains, mice were orally infected with 2×10^8 CFU of each strain. Three days after infection, Peyer's patches were isolated and a single-cell suspension was obtained by mechanical disruption through a cell mesh. Cells were incubated for 5 min in

erythrolysis buffer (7.8 mM NH_4Cl, 10 mM KHCO3, 100 μM EDTA) and then resuspended in PBS-FCS (1%). FcγR was blocked by a 5-min incubation with CD16/32 antibodies (1:50 dilution). CD3-phycoerythrin (PE), CD19-fluorescein isothiocyanate (FITC), F4/80-allophycocyanin (APC), CD11b-APC-A750, CD11c-peridinin chlorophyll protein-Cy5.5, and Ly6G-PE-Cy7 (clone 1A8) were purchased from BD Bioscience and titrated for optimal staining conditions (1:800, 1:200, 1:200, 1:500, 1:100, and 1:100, respectively). Surface markers were stained by a 30-min incubation at room temperature in PBS-FCS (1%). After staining, cells were washed twice and resuspended in 300 μl of PBS-FCS (1%). DAPI (1:10,000) was added to the samples immediately before loading them into an LSRII apparatus (BD Bioscience). Acquired data were analyzed with FlowJo software (Treestar). Data from three independent experiments were pooled together, and the population abundance was normalized to the average response induced by the wild-type strain YPIII.

RESULTS

Bioinformatic analysis of the InvA-like proteins. In the *Y. pseudotuberculosis* YPIII database, three additional monocistronic open reading frames (ORFs) with significant homology to the invasin (InvA) protein were identified, YPK_2513, YPK_0145, and YPK_1315 (Fig. 1A; also see Table S2 in the supplemental material). The YPK_2513 gene encodes a product of 1,075 amino acids (aa), including the signal sequence, and was originally named InvB to indicate its relationship to InvA. As InvB is equivalent to Ifp, which was recently identified in strain IP32953 (57), we also refer to InvB as Ifp. A very large InvA-type protein of 5,337 aa is encoded by the YPK_0145 gene, designated InvC, and YPK_1315 results in the production of a 1,976-aa protein, which we named InvD. All of the putative adhesins encode a highly homologous N-terminal β-barrel-like structure with about 40 to 46% similarity between aa 100 and 550, which are responsible for the incorporation of the invasin/intimin adhesins into the bacterial outer membrane (see Fig. S1 in the supplemental material). The Ifp, InvC, and InvD proteins are characterized by intermediate regions with 4, 47, or 13 repetitive Ig-like globular structures, respectively, and a unique C-terminal domain, but the repetitive sequences of the different InvA-type proteins are not related (Fig. 1B). A computational analysis revealed that the *ifp* and *invC* genes also are present in all other sequenced *Y. pseudotuberculosis* genomes (IP31758, IP32953, and PB1/+). The Ifp proteins are highly homologous (99% identity), whereas the InvC proteins vary significantly in repetitive sequence numbers. InvC proteins of PB1/+ and IP31758 have only 32 and 44 repeats, whereas InvC of IP32953 is the largest molecule, with 50 repetitive sequences (see Table S2). Interstrain alignments further showed that the *invD* gene is present in YPIII and IP31758 but not in PB1/+ and IP32953. The first 1,730 aa of the predicted InvD proteins of YPIII and IP31758 are highly homologous, but the following C-terminal domains vary significantly in amino acid sequence and length due to the presence of a different genetic element that replaced the last seven highly homologous Ig domains and the C-terminal C-type lectin domain with 246 unrelated amino acids with no homology to other gene sequences. Our computational analysis indicated that this variation is the result of a chromosomal rearrangement associated with the insertion of IS*1237* 155 bp downstream of the *invD* gene.

Based on this information, we focused our efforts on the analysis of the conserved *ifp* and *invC* gene products, which show a conserved chromosomal organization and are present in all available *Y. pseudotuberculosis* genomes, and we tested their effects on host tissue colonization and virulence.

Expression of *ifp* and *invC* in response to environmental conditions. Adhesive structures may be important for the colonization of surfaces in external habitats (plants and insects) or the mammalian host. To obtain more information about the role of the putative adhesins and their possible functions during the infection process, we first tested the expression profile of both adhesin genes in *Y. pseudotuberculosis* YPIII under various environmental conditions (e.g., minimal and complex media, various temperatures, and different growth phases) using *ifp-luxCDABE* and *invC-luxCDABE* reporter fusion strains. However, *ifp* and *invC* expression generally was very low under all tested laboratory growth conditions compared to the well-studied expression of the *invA* gene (data not shown; also see Fig. S2 in the supplemental material), which was maximally expressed at moderate temperature (25°C) during stationary phase (28, 44). The transcription of *ifp* and *invC* was slightly increased at 37°C, but overall expression was still low, e.g., similar to that of *invA* under repressing conditions. The expression of the *invA*-, *ifp*-, and *invC-luxCDABE* fusions was also analyzed in the *Y. pseudotuberculosis* wild-type strain IP32953 to test whether the transcription of the putative adhesin genes differs among strains with a slightly different repertoire of virulence genes (e.g., no *invD* gene; see Table S2). We found that the expression levels of the fusions are comparable between YPIII and IP32953 (data not shown).

Expression of *ifp* and *invC* in the murine infection model. As the transcription of both *ifp* and *invC* was low under *in vitro* growth conditions, we also tested the expression of the putative adhesin genes *in vivo* during infection in the mouse model. To do so, BALB/c mice were orally infected with 5×10^8 bacteria of the *Y. pseudotuberculosis* wild-type strain YPIII expressing an *invA*-, *ifp*-, or *invC-luxCDABE* reporter fusion construct, and the bioluminescent signal was monitored in living animals for 3 days using an *in vivo* imaging system. Although no luciferase activity could be measured in the bacterial suspension before and during early time points of the infection ($\leq$1 day) (Fig. 2), a bioluminescent signal of the *ifp* and *invC* luciferase reporter fusion was observed in the intestinal tract of the mice during later stages of infection (days 2 and 3) (Fig. 2). In contrast, a strong bioluminescent signal was detected in mice harboring the *invA-luxCDABE* fusion before and immediately after infection. The signal decreased after several hours but started to increase on days 2 and 3 (Fig. 2). In contrast, no light emission could be detected from mice infected with bacteria carrying the promoterless *luxCDABE* operon in an identical expression system. To address whether expression varies between different *Y. pseudotuberculosis* isolates, we also tested the expression of the *invA*-, *ifp*-, and *invC-luxCDABE* fusions in the *Y. pseudotuberculosis* strain IP32953 and found that a similar expression pattern was detectable during infection in the murine model (see Fig. S3 in the supplemental material).

To study *ifp* and *invC* expression in the infected tissues on the single-cell level, we used a developed set of fluorescent fusion vectors (62). YPIII harboring a plasmid-encoded constitutive P_{gapA}::*dsred2* fusion and a compatible P_{ifp}::$gfp_{mut3.1}$ or P_{invC}::$gfp_{mut3.1}$ reporter construct was used to infect BALB/c mice. Cryosections were prepared of the PPs, MLNs, and spleens 3 days postinfection. The bacteria in the tissues were visualized by monitoring dsRed2 and then tested for P_{ifp}::$gfp_{mut3.1}$ or P_{invC}::$gfp_{mut3.1}$ expression. As shown in Fig. 3, red fluorescent bacteria could easily be detected

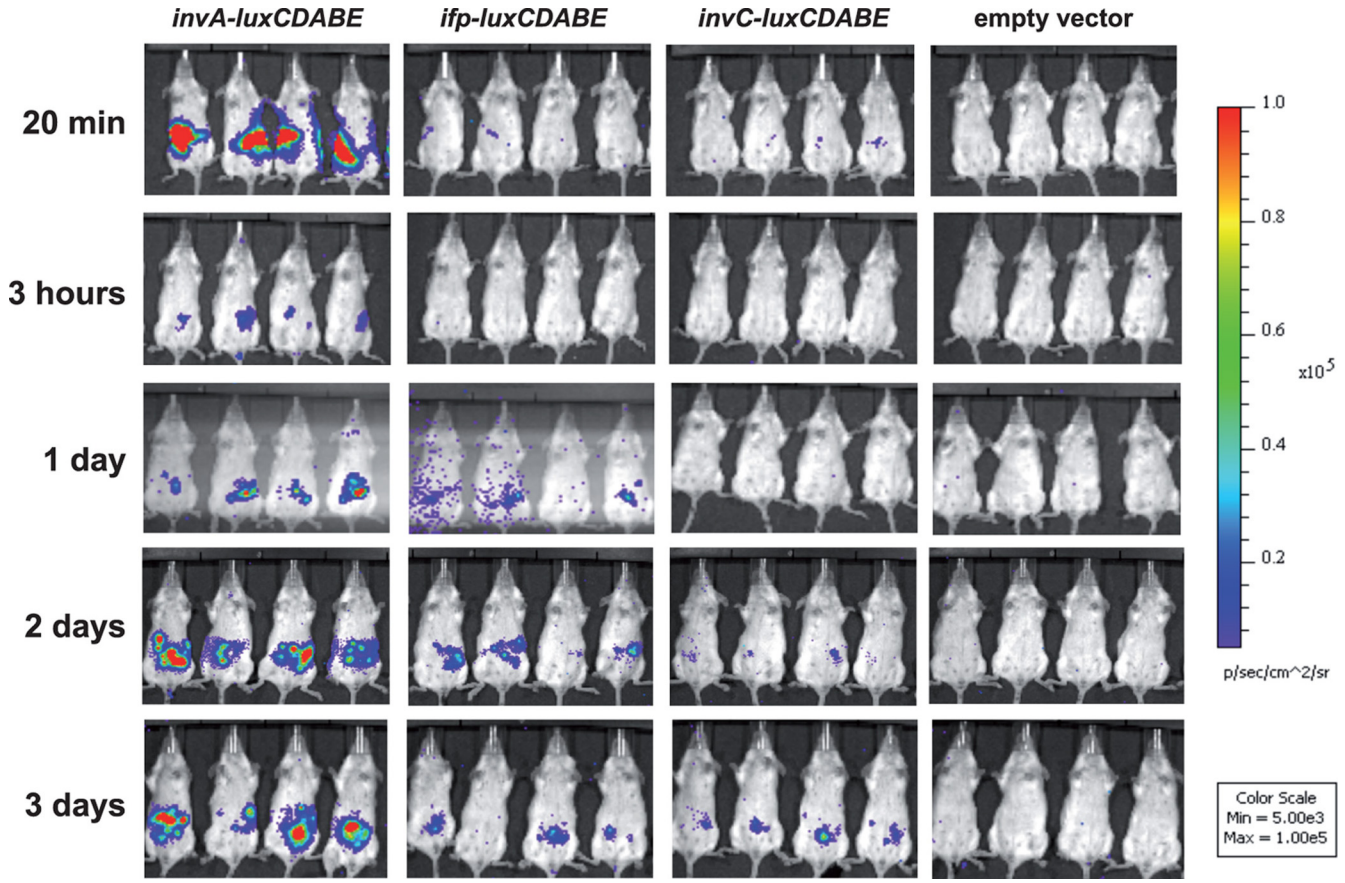

FIG 2 *In vivo* expression analysis of *invA*-, *ifp*-, and *invC-luxCDABE* fusions. Cells (5×10^8) of *Y. pseudotuberculosis* YPIII pFU98 (empty vector), YPIII pFU143 (P_{invA}::*luxCDABE*), YPIII pFU144 (P_{ifp}::*luxCDABE*), and YPIII pFU145 (P_{invC}::*luxCDABE*) were used to orally infect BALB/c mice. Mice were anesthetized at the indicated time points, and bioluminescence was detected with an IVIS camera on the ventral side.

within the lymphatic tissues. Both the P_{ifp}::$gfp_{mut3.1}$ and the P_{invC}::$gfp_{mut3.1}$ fusions were expressed in the bacteria localized in the PPs 3 days postinfection, but they were not expressed in the MLNs and spleen at this stage of infection.

Ifp and InvC promote adhesion to cultured intestinal cells. The *in vivo* expression analysis indicated that Ifp and InvC are important for the colonization of the intestinal tract during later stages of infection. For this reason, we wanted to find out whether the InvA-type proteins are able to promote binding to intestinal epithelial cells. As both proteins were not expressed in *Y. pseudotuberculosis* YPIII under various *in vitro* growth conditions, we cloned the genes under the arabinose-inducible BAD promoter (P_{BAD}) and expressed the proteins with and without a C-terminal His tag in *E. coli* K-12 and *Y. pseudotuberculosis* YPIII. The Ifp_{His6} and $InvC_{His6}$ derivatives were used to detect and optimize the expression of the putative adhesins and to demonstrate the proper insertion of the proteins into the *E. coli* and *Y. pseudotuberculosis* outer membrane (data not shown; also see Fig. S4 in the supplemental material).

We first analyzed the ability of Ifp and InvC to promote the attachment of nonadherent *E. coli* K-12 cells to human (Caco-2) (Fig. 4A), porcine (IPEC-J2) (Fig. 4B), and murine intestinal epithelial cells (Mode-K) (Fig. 4C). As it has previously been reported that an addition of only two additional amino acids can affect the adhesion and cell entry efficiency of the *Y. pseudotuberculosis* InvA protein (30), we used bacteria expressing the His- and non-His-tagged version of Ifp and InvC for the adhesion assays. In addition, we tested the capacity of Ifp- and InvC-producing bacteria to enter into the different epithelial cells by the gentamicin protection assay. For these studies, *E. coli* K-12 pRI203 expressing the well-characterized adhesin InvA was used as a positive control for cell attachment and entry. As shown in Fig. 4, Ifp-expressing *E. coli* exhibited a significantly higher binding ability to human, porcine, and murine intestinal cells than *E. coli* harboring the empty vector plasmid. An increase of cell attachment also was found for InvC-expressing bacteria, although InvC-mediated adhesion to the different intestinal cells generally was less efficient than that of Ifp (Fig. 4). Cell binding by both His-tagged adhesins was not reduced compared to that of the nontagged derivatives, indicating that additional amino acids have no negative influence on the cell binding capacity of the proteins. Furthermore, we found that Ifp-expressing *E. coli* was able to internalize into Caco-2 cells (6%), but entry efficiency was lower than that of the cell uptake of *E. coli* expressing the InvA protein (24%). In contrast, the InvC-overexpressing *E. coli* cells were unable to promote host cell entry (Fig. 4).

We also assessed the adhesive and invasive functions of Δ*ifp* and Δ*invC* mutant strains, but the inactivation of both adhesin genes had no significant effect on cell adhesion and uptake when grown in bacterial complex or minimal media, at 25 or 37°C, to

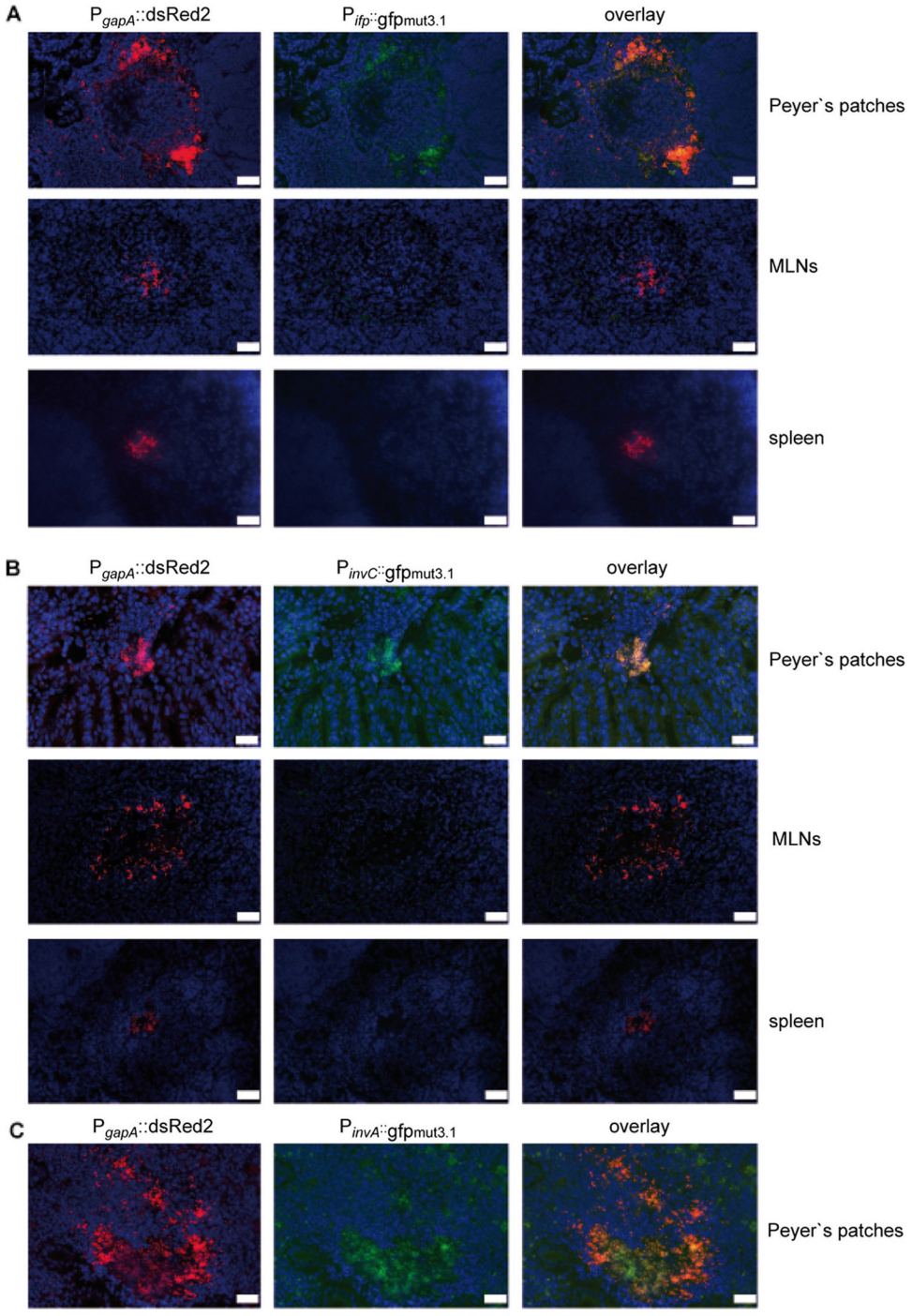

FIG 3 Expression of P_{ifp}::*gfp* and P_{invC}::*gfp* fusions in PPs and MLNs. Cells (2×10^8) of *Y. pseudotuberculosis* YPIII pFU147 (P_{ifp}::*gfp* $_{mut3.1}$) (A) and YPIII pFU148 (P_{invC}::$gfp_{mut3.1}$) (B) were used to orally infect BALB/c mice. Three days postinfection mice were sacrificed, and PPs and MLNs were isolated. Histological slides were prepared and analyzed by fluorescence microscopy to detect bacteria in the tissues by the expression of the reporter protein DsRed2. In parallel, *ifp* and *invC* expression in the bacteria was monitored by GFPmut3.1-mediated fluorescence. White bars indicate 20 μm. (C) Peyer's patches of mice infected with *Y. pseudotuberculosis* YPIII pFU146 (P_{invA}::*gfp* $_{mut3.1}$) were used as a control.

exponential or stationary phase (data not shown). This may be explained by the low *in vitro* expression of both *inv* genes under these growth conditions (see Fig. S2 in the supplemental material) and the presence of other efficient adhesins, e.g., InvA and YadA, which could compensate for the loss of adhesive functions. To demonstrate cell binding to epithelial cells by Ifp and InvC in *Y. pseudotuberculosis*, we introduced the Ifp and InvC expression constructs into the *invA* mutant strain YP9 and analyzed their ability to enhance the cell attachment and invasion of the transformants grown at 25°C, conditions under which *yadA* is not expressed. As shown in Fig. 5A, the overall adhesion of *Y. pseudotuberculosis* was reduced 2-fold in the absence of InvA, but the

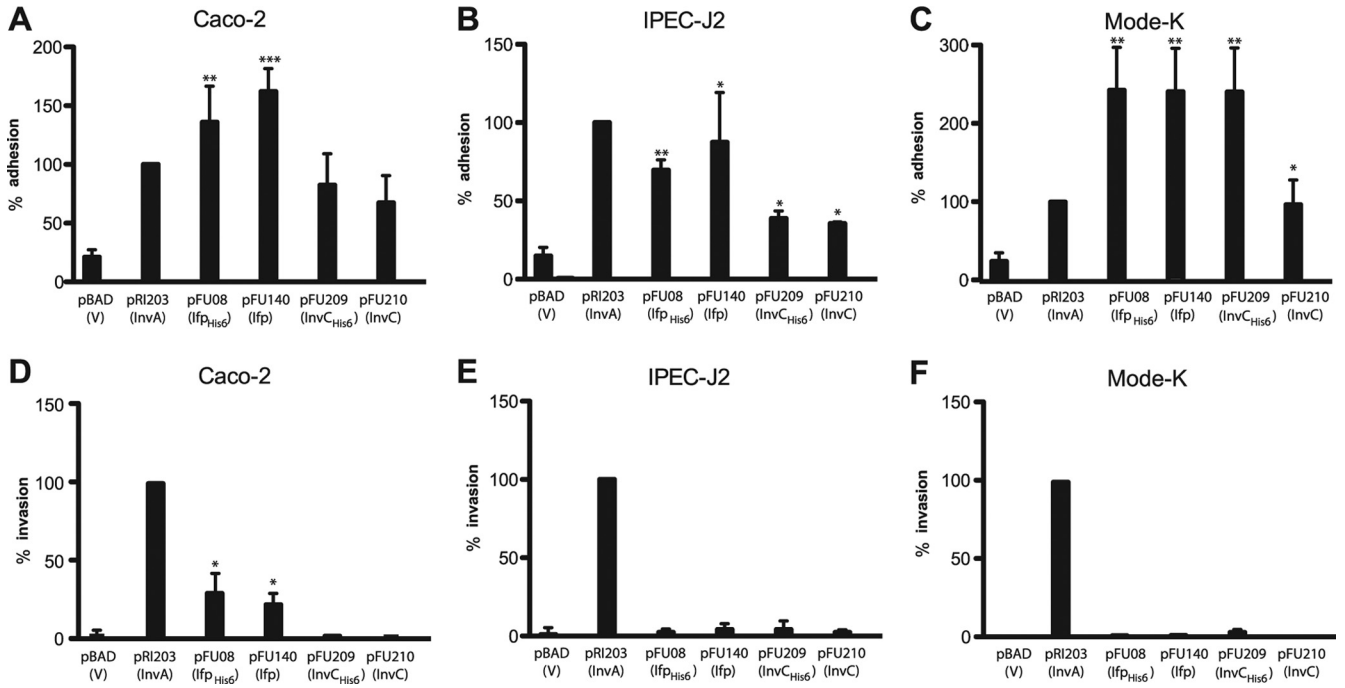

FIG 4 Ifp- and InvC-expressing *E. coli* K-12 mediate interaction with epithelial cells. Cell adhesion (A to C) and invasion (D to F) efficiencies of the *E. coli* strains expressing InvA (DH10β pRI203), Ifp (DH10β pFU08), Ifp$_{His6}$ (DH10β pFU140), InvC (DH10β pFU209), and InvC$_{His6}$ (DH10β pFU210) were determined with human enterocytes (Caco-2) (A and D), pig-derived cells (IPEC-J2) (B and E), or mouse-derived intestinal cells (Mode-K) (C and F). *E. coli* harboring the empty vector plasmid pBADmycA was used as a negative control. About 5×10^6 bacteria were used to challenge 5×10^4 cells, and they were incubated for 30 min at 20°C to determine cell attachment or at 37°C to monitor invasion efficiency. The total numbers of adherent and internalized bacteria were determined as described in Materials and Methods. The data are presented as means ± standard deviations from three independent experiments performed in triplicate. Data were analyzed by the Student's *t* test. Asterisks indicate results that differed significantly from those for YPIII pBADmycA: *, $P < 0.05$; **, $P < 0.01$; ***, $P < 0.001$.

overexpression of *ifp* compensated for this loss and enhanced HEp-2 binding by about 2.5-fold. The production of InvC did not significantly alter the overall adhesive and invasive properties of the *invA* mutant (Fig. 5B) and supported previous results showing that cell interactions promoted by Ifp are stronger than adherence by InvC (Fig. 4).

Since both *in vivo* expression and *in vitro* host cell interaction analyses suggested a role of Ifp and InvC in intestinal colonization, we also used differentiated Caco-2 cells that formed a tight polarized monolayer that was more reminiscent of the physiological situation of the intestinal epithelium. First, Ifp- and InvC-expressing *E. coli* cells were added to the monolayer, nonadherent bacteria were removed by washing, and the infected monolayers were analyzed by scanning electron microscopy. As shown in Fig. 5B, only single *E. coli* cells expressing InvC were detected on polarized Caco-2 cells, whereas multiple microcolonies of adherent Ifp-producing *E. coli* could be identified. This indicated that Ifp leads to bacterial aggregation and mediates efficient interaction with differentiated human intestinal cells. We also used YPIII and the isogenic Δ*ifp* and Δ*invC* mutant strains for monolayer infection and quantified the number of adherent and internalized bacteria after 3 h of infection (Fig. 5C and D). In support of previous data, the Δ*ifp* mutant (YP97) exhibited a significant decrease in its binding and invading ability compared to that of the wild type, whereas no significant difference between the Δ*invC* mutant and the wild-type strain was detected. We also introduced an *ifp*$^+$ plasmid (pFU234) into the Δ*ifp* mutant (YP97) and used the resulting strain for monolayer infections. The adhesion and invasion of this strain were comparable to those of the *Y. pseudotuberculosis* wild-type strain YPIII (Fig. 5C and D). The presence of the empty expression vector pFU109 had no effect on the cell binding and invasion properties (data not shown). This demonstrated that the plasmid-carried *ifp* gene is able to complement the adhesion and invasion phenotype of the *ifp* mutation.

Ifp and InvC effects on virulence. To assess the effects of Ifp and InvC on *Y. pseudotuberculosis* pathogenesis, we tested the virulence of the wild-type and mutant strains in the murine infection model. Two different age groups of BALB/c mice were orally infected with 2×10^9 bacteria of the wild-type strain (YPIII) or the isogenic Δ*ifp* (YP97) or Δ*invC* (YP98) mutant. As shown in Fig. 6, all mice infected with either the wild type or the *inv* mutants succumbed to infection; however, the survival of mice infected with the *ifp*-deficient strain was slightly prolonged in 7-week-old mice. Overall, the phenotype of the *ifp* and *invC* mutants was not dramatic, as indicated by the limited differences observed between the wild type and the knockout mutants, but the infection seems altered in the absence of Ifp.

To further analyze the influence of Ifp and InvC on the progress of an infection, mice were orally infected with 2×10^8 YPIII, YP97 (Δ*ifp*), or YP98 (Δ*invC*) bacteria. After 3 days, the CFU in the small intestine, the PPs, the MLNs, liver, and spleen was quantified (see Fig. S5 in the supplemental material). The number of the *ifp* and *invC* mutant strains recovered from the host tissues was not significantly different from that for the wild-type strain, indicating that the presence of remaining colonization factors is suf-

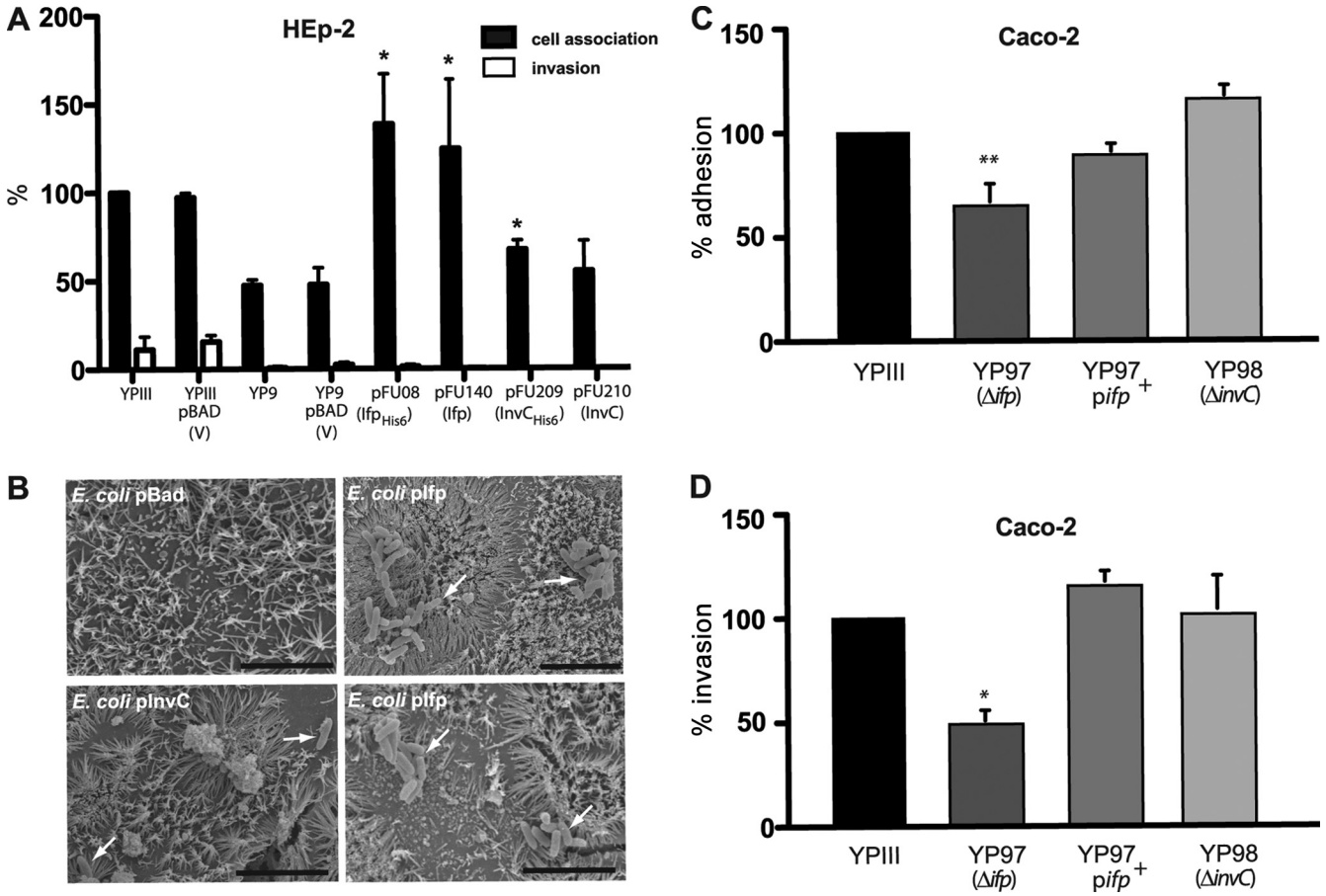

FIG 5 Ifp complements cell adhesion function of InvA. (A) Cell adhesion and invasion efficiencies of *Y. pseudotuberculosis* YP9 (Δ*invA*) expressing Ifp (pFU08), Ifp_{His6} (pFU140), InvC (pFU209), or $InvC_{His6}$ (pFU210) were determined with human epithelial cells. Strains harboring the empty vector plasmid pBADmycA were used as a negative control. About 5×10^6 bacteria were used to challenge 5×10^4 cells, and the samples were incubated for 30 min at 20°C to determine cell attachment or at 37°C to monitor invasion efficiency. The data are presented as means ± standard deviations from three independent experiments performed in triplicate. Data were analyzed by the Student's *t* test. Asterisks indicate results that differed significantly from those for YPIII pBADmycA ($P < 0.05$). (B) *E. coli* K-12 cells harboring the empty vector pBAD-Myc, pFU140 (Ifp^+), or pFU210 ($InvC^+$) were used to infect polarized Caco-2 cells. Adherent bacteria were visualized by scanning electron microscopy and are indicated by white arrows. The black bars indicate 5 μm. (C and D) Monolayers of differentiated Caco-2 cells were challenged with YPIII, YP97 (Δ*ifp*), and YP98 (Δ*invC*) and incubated for 3 h at 25 and 37°C to monitor cell attachment (C) and invasion (D). The total numbers of adherent and internalized bacteria were determined as described in Materials and Methods. The data represent the means ± standard deviations from three independent assays done in triplicate. Data were analyzed by the Student's *t* test. The asterisks indicate results that differed significantly from those for YPIII: *, $P < 0.05$; **, $P < 0.01$.

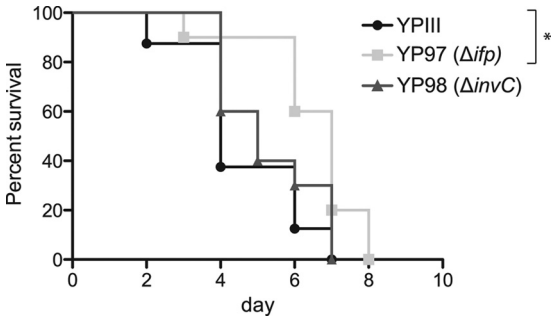

FIG 6 Survival of mice infected with YPIII or the *ifp*- and *invC*-deficient mutants. Cells (2×10^9) of *Y. pseudotuberculosis* wild-type strain YPIII or the *ifp* (YP97) and *invC* (YP98) mutant strains were orally introduced into 7-week-old BALB/c mice. The survival of BALB/c mice was monitored for up to 14 days. Data were analyzed by the log-rank (Mantel-Cox) test. Asterisks indicate results that differed significantly from those for YPIII ($P < 0.05$).

ficient for a successful infection. To further define the role of Ifp and InvC during infection, we also performed coinfection experiments with wild-type and mutant strains to minimize inherent interanimal variations to detect even subtle differences in the colonization of host tissues. Groups of BALB/c mice were orally infected with 2×10^8 bacteria in an inoculum comprised of an equal mixture of the wild type and the isogenic mutant strain YP97 (Δ*ifp*) or YP98 (Δ*invC*), and the bacterial burden in the PPs, MLNs, liver, and spleen was determined 3 days postinfection (Fig. 7). Significantly lower numbers of *ifp*-deficient mutant bacteria were recovered from the small intestine, PPs, and MLNs, and much smaller amounts of this mutant were isolated from liver and spleen. The calculation of the competitive index of the mutant relative to that of the wild-type strain indicated that higher levels of Ifp during mouse infections are advantageous for the colonization of all analyzed host tissues (Fig. 7). InvC had only a minor effect on pathogenesis compared to that of Ifp. The colonization

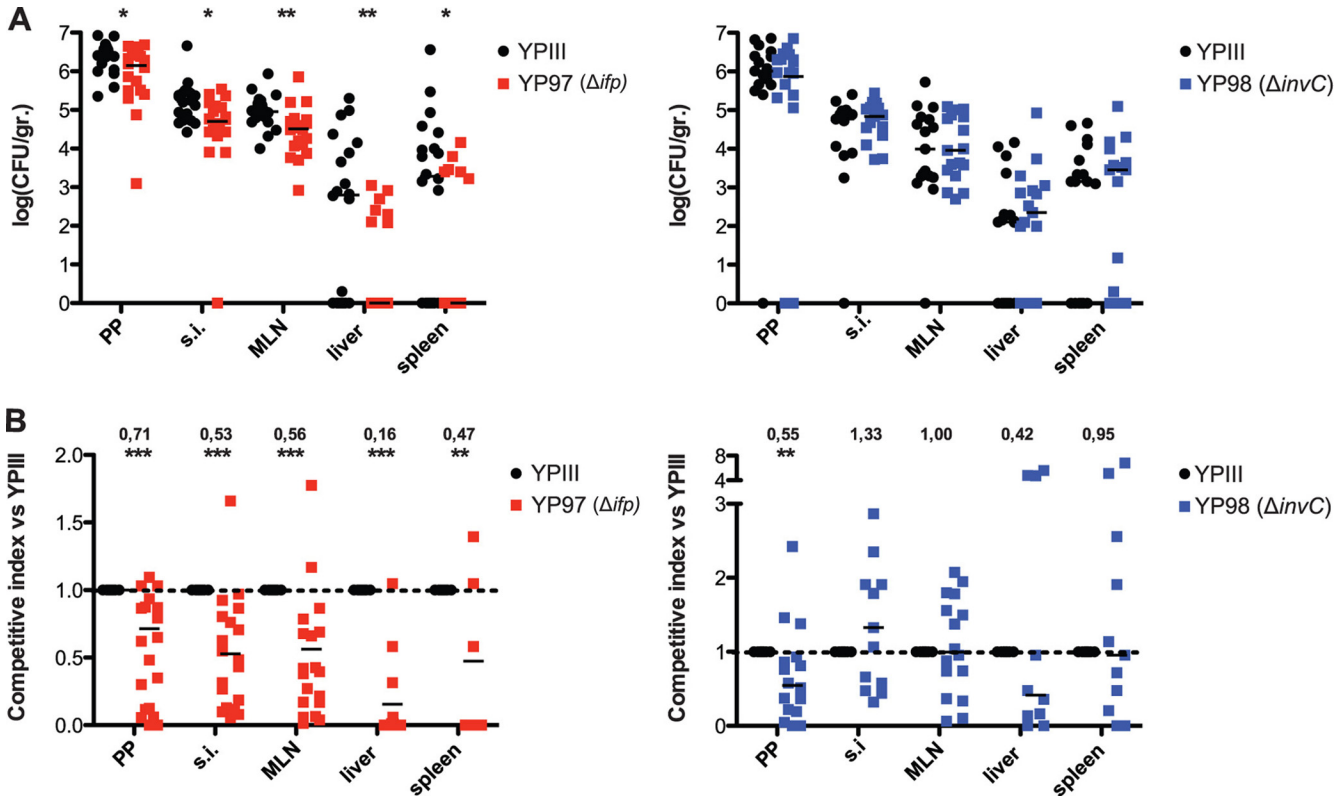

FIG 7 Influence of Ifp and InvC on the colonization of intestinal lymphatic tissues and organs. (A) BALB/c mice were coinfected via the orogastric route with 2×10^8 bacteria in an inoculum comprised of an equal mixture of *Y. pseudotuberculosis* YPIII (wt) and YP97 (Δ*ifp*) or YP98 (Δ*invC*). Three days postinfection, the mice were sacrificed and the numbers of surviving bacteria in the small intestine (SI), PPs, MLNs, liver, and spleen determined as described in Materials and Methods. Data are presented as a scatter plot of numbers of CFU per gram of organ as determined by counts of viable bacteria on plates. Each spot represents the CFU count in the indicated tissue samples from one mouse. The levels of statistical significance for differences between test groups were determined by the Mann-Whitney test. Asterisks indicate results that differed significantly from those for YPIII: *, $P < 0.05$; **, $P < 0.01$. (B) Data are graphed as competitive index values for the tissue samples from one mouse. The bars represent the medians of the competitive index values. A competitive index score of 1 denotes no difference in virulence compared to that of YPIII. Asterisks indicate results that differed significantly from those for YPIII: **, $P < 0.01$; ***, $P < 0.001$.

of the *invC* mutant strain generally was very similar to that of the wild type and was only slightly reduced in the PPs, indicating that InvC plays no major role for virulence in mice.

To confirm the effect of Ifp, we also analyzed the colonization of the wild type and the complemented *ifp* mutant strain. In contrast to the YPIII/YP97 coinfection experiment, similar numbers of both strains were recovered from infected tissues and organs, indicating that the loss of *ifp* can be complemented by a plasmid-carried copy of the adhesin gene (see Fig. S6 in the supplemental material). To address whether the contribution of Ifp to virulence can also be observed in other *Y. pseudotuberculosis* isolates, we performed coinfection experiments with *Y. pseudotuberculosis* IP32953 and its isogenic Δ*ifp* mutant derivative IP32953 ΔIFP (57). Similarly, lower numbers of the *ifp*-deficient IP32953 strain were recovered from gut-associated lymphatic tissues, liver, and spleen (see Fig. S7), indicating that the presence of Ifp also is advantageous for the colonization of other *Y. pseudotuberculosis* isolates. However, the effect of Ifp on the virulence of IP32953 seemed slightly less than that of YPIII.

Loss of Ifp and InvC leads to an enhanced recruitment of professional phagocytes in the PPs. From many studies it is known that the coordinated activity of neutrophils (polymorphonuclear leukocytes [PMNs]), dendritic cells (DCs), and macrophages (mononuclear monocytes) constitutes the body's first line of defense against intruding pathogens. Neutrophils and macrophages are abundant circulating leukocytes, and the histological analysis of PPs from mice infected with YPIII demonstrated an accumulation of these phagocytes at the periphery of the follicles or in the infected necrotic areas of the PPs (41).

To elucidate whether the loss of the Ifp and InvC adhesins provokes a more extensive and/or progressed immune response at this time point of infection, we isolated the PPs from mice 3 days postinfection with YPIII, YP97 (Δ*ifp*), or YP98 (Δ*invC*) and analyzed the cell type composition via fluorescence-activated cell sorter (FACS) analyses. The antibodies used for this experiment were chosen to determine defined populations of different lymphocytes (T cells, $CD3^+$; B cells, $CD19^+$), macrophages ($CD11^+$and $F4/80^+$), and neutrophils ($Ly6G^+$), as well as populations of dendritic cells ($CD11c^+$). As shown in Fig. 8, very low numbers of professional phagocytes were identified in the PPs of uninfected mice, whereas a massive recruitment of these immune cells was seen 3 days postinfection. Further analysis of the recruited/persistent cell population demonstrated that macrophages and/or neutrophils in particular and, to a lower extent, dendritic cells, are recruited into the infected lymph follicles, whereas the number of T and B cells remained constant (Fig. 8). Comparison with the two adhesins mutants further revealed that a significantly higher number of these immune cells, particularly

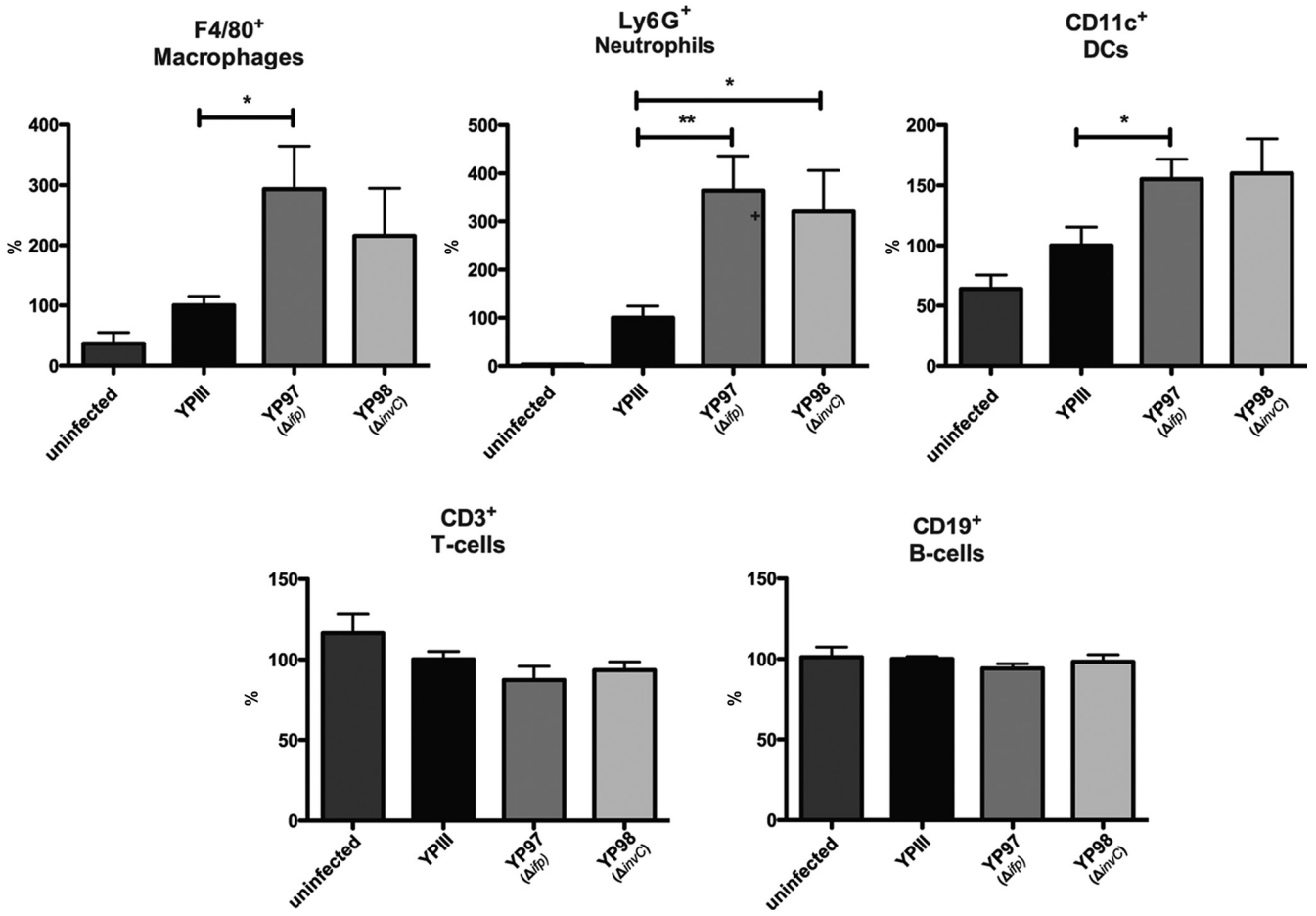

FIG 8 Analysis of immune cells recruited to PPs after infection with *Y. pseudotuberculosis* YPIII or the *ifp* and *invC* mutant. About 2×10^8 bacteria (YPIII, YP97, and YP98) were used to infect 10 BALB/c mice per strain. Three days after infection mice were sacrificed, PPs were isolated and homogenized, and the cell suspensions were used for FACS analysis. Values on the *y* axis indicate the percentage of cells relative to the cells isolated from PPs infected with the wild-type strain YPIII. F4/80$^+$, macrophages; Ly6G$^+$ (1A8 clone), neutrophils; CD11c$^+$, dendritic cells; CD3$^+$, T cells; CD19$^+$, B cells. Asterisks indicate results that differed significantly from those for YPIII: *, $P < 0.05$; **, $P < 0.01$.

macrophages and neutrophils, were recruited and/or retained in the PPs after infection with the *ifp* mutant strain (Fig. 8). An increase of professional phagocytes also was found after infection with the *invC* mutant, although the overall number of attracted immune cells was lower and significant only for neutrophils. This demonstrated that the penetration and/or persistence of the *ifp*- and *invC*-deficient *Y. pseudotuberculosis* strains in the PPs is reduced, and this is accompanied by an increase of professional phagocytes.

DISCUSSION

The colonization of the interior surface of the intestine by enteropathogenic *Yersinia* spp. is an essential step in the process of an infection, and the adhesion factors invasin and YadA were shown to play an especially crucial role in this process (23, 26, 39, 64). However, recent genome analyses revealed that pathogenic yersiniae encode a substantial number of additional proteins with significant homology to these well-characterized *Yersinia* adhesins. In this study, we characterized the *in vivo* synthesis and function of two invasin-type proteins, named Ifp and InvC, and showed that they promote the association of *Y. pseudotuberculosis* with intestinal epithelial cells and affect colonization in the Peyer's patches of mice.

Both proteins are highly homologous to the invasin/intimin family of outer membrane proteins. Notably, InvC also comprises an N-terminal LysM-type domain. This domain can be found in peptidoglycan-degrading enzymes (autolysins) and is predicted to bind peptidoglycan (3, 56). It might act as an additional base to stabilize the β-barrel autotransport structure of the large surface-exposed portion of InvC (60). Alternatively, the LysM-type domain might be implicated in the translocation of the outer membrane protein through the cross-linked peptidoglycan layer (50).

In contrast to invasin (InvA), Ifp and InvC of *Y. pseudotuberculosis* YPIII are not produced under *in vitro* cultivation conditions. However, *in vivo* expression analyses demonstrated that both adhesin genes are induced in the PPs of mice but not in the MLNs and spleen during later stages of the infection. This indicated that both genes are activated in response to specific environmental signals sensed in gut-associated tissues. Such a fine-tuned expression of the adhesins during the infection process enables the bacteria to adjust cell binding and detachment to allow colonization and dissemination to other host sites (58).

Cell culture infection experiments with Ifp- and InvC-expressing *E. coli* demonstrated that both proteins promote tight

adherence to human, porcine, and murine intestinal cells. Furthermore, Ifp was shown to be able to promote low-efficiency uptake into human enterocytes, and this ability seems to be enhanced when the intestinal cells are polarized in a monolayer system. The observation that the uptake of the *ifp*-deficient strain IP32953 (ΔIFP) into HEp-2 cells was reduced by 20 to 25% supports a role of this Inv-type protein as an invasin (57). However, when we compared the attachment of *Y. pseudotuberculosis* YPIII to HEp-2 cells to that of the isogenic *ifp*- and *invC*-deficient strains, we were unable to detect a reduction of the cell binding and entry capacities of the mutant strains. This result may reflect (i) the weak expression of both adhesin genes *in vitro* and (ii) the presence of other highly efficient cell adhesion factors which fully compensate for the loss of Ifp and InvC in YPIII but may not do so in IP32953. In fact, the absence of the *invA* gene reduced overall binding and invasion into epithelial cells, and this defect could be restored by the overexpression of the Ifp protein. Moreover, the loss of Ifp reduced the internalization of YPIII into differentiated human enterocytes in which the expression of the invasin receptors (β_1-integrins) is repressed (33). This finding indicates that Ifp is important for host colonization under conditions in which invasin expression and/or function is reduced.

Strong et al. used an insect model (*Galleria mellonella*) to study the influence of the Ifp protein of *Y. pseudotuberculosis* IP32953 and found a moderate attenuation compared to its expression in the wild type (57). In this study, we used the traditional murine yersiniosis infection model to examine the influence of Ifp and InvC of *Y. pseudotuberculosis* YPIII on virulence in mammals. The survival of mice was slightly prolonged in the absence of Ifp, and a more in-depth mouse infection analysis showed that Ifp plays a role in *Y. pseudotuberculosis* pathogenesis by promoting invasion and/or replication in lymphatic tissues and organs. This is supported by the fact that *ifp* is encoded by all known *Y. pseudotuberculosis* genomes, but it is inactivated by insertion sequences or stop mutations, similarly to the *invA* gene, in all available *Y. pestis* genomes (10, 14, 34, 57). The presence of the InvC adhesin seems less important for virulence in mice via the oral route, although the *invC* adhesin gene is also present in all *Y. pseudotuberculosis* strains. Based on the large number of known and predicted adhesin proteins, it is highly likely that other adhesive factors of the bacteria compensate for the loss of InvC function during infection. A more complex analysis of mutants deficient in two or more adhesin factors would be required to elucidate the contribution of individual factors to the invasion and dissemination process. Interestingly, InvC homologues also are found in *Y. pestis* genomes with various numbers of the repetitive Ig-like domains in the intermediate passenger region (10, 14, 34, 57). As *Y. pestis* is able to invade host cells but does not produce any of the characterized invasins of the enteropathogenic *Yersina* species (InvA, Ifp, YadA, and Ail), it would be interesting to know whether this adhesion factor plays a more important role for *Y. pestis* pathogenesis.

Improved adhesion to the intestinal epithelium promoted by Ifp could allow better penetration of the PPs and dissemination to deeper tissues. A previous study nicely demonstrated that *Y. pseudotuberculosis* disseminates to the liver and spleen by two distinct translocation events (2). Shortly after infection, the bacteria translocate across M cells, enter intestinal lymph tissues, and are spread to the organs, from which they are quickly eliminated. After replication in the intestinal lumen, a second translocation event occurs which initiates late-stage extraintestinal dissemination to liver and spleen independently of the regional lymph nodes (2). A strong connection between the intestinal growth of bacteria and successful dissemination argues that the second translocation event is promoted by bacterial factors induced during later stages of infection. Here, we demonstrate that the Ifp adhesin is produced only after prolonged growth in the mouse intestine. Furthermore, it promotes tight adhesion and internalization into differentiated enterocytes, and it is required for the efficient colonization of liver and spleen. This makes Ifp an ideal candidate for an alternative portal that allows the transportation of the bacteria out of the intestine.

Upon the entry of *Y. pseudotuberculosis* YPIII into PPs, the bacteria induce immune responses which are characterized by an inflammation with the infiltration of macrophages and neutrophils. They also cause pyogenic lesions that are thought to result from the elimination by nonspecific cellular mechanisms, e.g., attracted neutrophils and macrophages. PPs of mice infected with *Y. enterocolitica* had a similar appearance, with the predominant recruitment of neutrophils and macrophages accompanied by cell death and necrotic tissue at the center of each focus (1, 49). Immunophenotyping showed that the number of neutrophils within the PPs in particular is significantly increased in the *ifp* and *invC* mutant strains. Variations in this cell population may result from differences in the first immunological response, e.g., the production of proinflammatory cyto- and chemokines, following a *Y. pseudotuberculosis* infection. The production of KC and tumor necrosis factor alpha (TNF-α), both implicated in neutrophil and macrophage recruitment, was previously shown to increase in the PPs during a *Yersinia* infection (22, 41). Part of the *Yersinia*-induced cytokine production is attributed to the activity of invasin or YadA. The binding of invasin or YadA leads directly to the expression of proinflammatory cytokines, including interleukin-8 (IL-8) (18, 31, 53, 61). Host cell contact promoted by longer Inv-type proteins in the PPs may prevent or reduce InvA/YadA-mediated cell contacts, characterized by lower KC secretion and reduced infiltration by macrophages and neutrophils. The adhesin(s) may also reduce the recognition of other immunogenic surface molecules, e.g., lipopolysaccharides, by the host immune system. Furthermore, yersiniae express a variety of different pathogenicity factors (Yop effectors) which are translocated into immune cells to reduce cyto- and chemokine production and evade the innate immune response (11, 63). Beuscher et al. showed that TNF-α production is actively suppressed in BALB/c mice during the very late stages of infection. This is due to several injected Yop proteins, e.g., YopB, YopP/J, and LcrV (4, 12, 55). Other Yop effectors (YopE and YopH) prevent the phagocytosis of the bacteria by macrophages and neutrophils or induce the apoptosis of the phagocytes (YopP/J) (11, 42, 63). Intimate host cell attachment is required for the efficient translocation of the Yop proteins by the type III secretion machinery, and this can be mediated by different surface adhesins. Ifp and InvC might contribute to this process in the PPs and support Yop-mediated defenses against attacks by the innate immune system.

In summary, the invasin-type proteins Ifp and InvC seem to represent two additional adhesins of *Y. pseudotuberculosis* which are primarily expressed in the PPs during later stages of infection. Ifp in particular seems to support the host colonization of the lymphatic tissues and organs, most likely by promoting host cell association and immune evasion strategies.

ACKNOWLEDGMENTS

We thank Ann Kathrin Heroven and Martin Fenner for helpful discussions and the critical reading of the manuscript. We also thank Brendan Wren for sharing unpublished results, for helpful discussions, and for providing us with the *Y. pseudotuberculosis* wild-type strain IP32953 and the isogenic *ifp* mutant derivative (IP32953 Δ*ifp*). Furthermore, we thank Jonas Zantow for experimental support, Stefan Lienenklaus for help with the IVIS camera system, and Sascha Cording for his help with the FACS analysis.

This work was supported by grants from the Deutsche Forschungsgemeinschaft (SFB621, Project B10) and the BMBF (Consortium FBI-Zoo), as well as the Fonds der Deutschen Chemie.

REFERENCES

1. **Autenrieth IB, Vogel U, Preger S, Heymer B, Heesemann J.** 1993. Experimental *Yersinia enterocolitica* infection in euthymic and T-cell- deficient athymic nude C57BL/6 mice: comparison of time course, histomorphology, and immune response. Infect. Immun. **61**:2585–2595.
2. **Barnes PD, Bergman MA, Mecsas J, Isberg RR.** 2006. *Yersinia pseudotuberculosis* disseminates directly from a replicating bacterial pool in the intestine. J. Exp. Med. **203**:1591–1601.
3. **Bateman A, Bycroft M.** 2000. The structure of a LysM domain from *E. coli* membrane-bound lytic murein transglycosylase D (MltD). J. Mol. Biol. **299**:1113–1119.
4. **Beuscher HU, Rodel F, Forsberg A, Rollinghoff M.** 1995. Bacterial evasion of host immune defense: *Yersinia enterocolitica* encodes a suppressor for tumor necrosis factor alpha expression. Infect. Immun. **63**:1270–1277.
5. **Biedzka-Sarek M, Jarva H, Hyytiainen H, Meri S, Skurnik M.** 2008. Characterization of complement factor H binding to *Yersinia enterocolitica* serotype O:3. Infect. Immun. **76**:4100–4109.
6. **Biedzka-Sarek M, Venho R, Skurnik M.** 2005. Role of YadA, Ail, and lipopolysaccharide in serum resistance of *Yersinia enterocolitica* serotype O:3. Infect. Immun. **73**:2232–2244.
7. **Bliska JB, Copass MC, Falkow S.** 1993. The *Yersinia pseudotuberculosis* adhesin YadA mediates intimate bacterial attachment to and entry into HEp-2 cells. Infect. Immun. **61**:3914–3921.
8. **Bolin I, Norlander I, Wolf-Watz H.** 1982. Temperature-inducible outer membrane protein of *Yersinia pseudotuberculosis* and *Yersinia enterocolitica* is associated with the virulence plasmid. Infect. Immun. **37**:506–512.
9. **Bottone EJ.** 1997. *Yersinia enterocolitica*: the charisma continues. Clin. Microbiol. Rev. **10**:257–276.
10. **Chain PS, et al.** 2004. Insights into the evolution of *Yersinia pestis* through whole-genome comparison with *Yersinia pseudotuberculosis.* Proc. Natl. Acad. Sci. U. S. A. **101**:13826–13831.
11. **Cornelis GR.** 2002. The *Yersinia* Ysc-Yop "type III" weaponry. Nat. Rev. Mol. Cell Biol. **3**:742–752.
12. **Cornelis GR.** 2002. *Yersinia* type III secretion: send in the effectors. J. Cell Biol. **158**:401–408.
13. **Datsenko KA, Wanner BL.** 2000. One-step inactivation of chromosomal genes in *Escherichia coli* K-12 using PCR products. Proc. Natl. Acad. Sci. U. S. A. **97**:6640–6645.
14. **Deng W, et al.** 2002. Genome sequence of *Yersinia pestis* KIM. J. Bacteriol. **184**:4601–4611.
15. **Derbise A, Lesic B, Dacheux D, Ghigo JM, Carniel E.** 2003. A rapid and simple method for inactivating chromosomal genes in *Yersinia.* FEMS Immunol. Med. Microbiol. **38**:113–116.
16. **Dersch P, Isberg RR.** 2000. An immunoglobulin superfamily-like domain unique to the *Yersinia pseudotuberculosis* invasin protein is required for stimulation of bacterial uptake via integrin receptors. Infect. Immun. **68**:2930–2938.
17. **Eitel J, Dersch P.** 2002. The YadA protein of *Yersinia pseudotuberculosis* mediates high-efficiency uptake into human cells under environmental conditions in which invasin is repressed. Infect. Immun. **70**:4880–4891.
18. **Eitel J, Heise T, Thiesen U, Dersch P.** 2005. Cell invasion and IL-8 production pathways initiated by YadA of *Yersinia pseudotuberculosis* require common signalling molecules (FAK, c-SRC, Ras) and distinct cell factors. Cell Microbiol. **7**:63–77.
19. **El Tahir Y, Skurnik M.** 2001. YadA, the multifaceted *Yersinia* adhesin. Int. J. Med. Microbiol. **291**:209–218.
20. **Frankel G, Candy DC, Everest P, Dougan G.** 1994. Characterization of the C-terminal domains of intimin-like proteins of enteropathogenic and enterohemorrhagic *Escherichia coli*, *Citrobacter freundii*, and *Hafnia alvei.* Infect. Immun. **62**:1835–1842.
21. **Hamburger ZA, Brown MS, Isberg RR, Bjorkman PJ.** 1999. Crystal structure of invasin: a bacterial integrin-binding protein. Science **286**:291–295.
22. **Handley SA, Dube PH, Revell PA, Miller VL.** 2004. Characterization of oral *Yersinia enterocolitica* infection in three different strains of inbred mice. Infect. Immun. **72**:1645–1656.
23. **Heise T, Dersch P.** 2006. Identification of a domain in *Yersinia* virulence factor YadA that is crucial for extracellular matrix-specific cell adhesion and uptake. Proc. Natl. Acad. Sci. U. S. A. **103**:3375–3380.
24. **Hoiczyk E, Roggenkamp A, Reichenbecher M, Lupas A, Heesemann J.** 2000. Structure and sequence analysis of *Yersinia* YadA and *Moraxella* UspAs reveal a novel class of adhesins. EMBO J. **19**:5989–5999.
25. **Isberg RR.** 1989. Determinants for thermoinducible cell binding and plasmid-encoded cellular penetration detected in the absence of the *Yersinia pseudotuberculosis* invasin protein. Infect. Immun. **57**:1998–2005.
26. **Isberg RR, Falkow S.** 1985. A single genetic locus encoded by *Yersinia pseudotuberculosis* permits invasion of cultured animal cells by *Escherichia coli* K-12. Nature **317**:262–264.
27. **Isberg RR, Leong JM.** 1990. Multiple beta 1 chain integrins are receptors for invasin, a protein that promotes bacterial penetration into mammalian cells. Cell **60**:861–871.
28. **Isberg RR, Swain A, Falkow S.** 1988. Analysis of expression and thermoregulation of the *Yersinia pseudotuberculosis inv* gene with hybrid proteins. Infect. Immun. **56**:2133–2138.
29. **Isberg RR, Voorhis DL, Falkow S.** 1987. Identification of invasin: a protein that allows enteric bacteria to penetrate cultured mammalian cells. Cell **50**:769–778.
30. **Isberg RR, Yang Y, Voorhis DL.** 1993. Residues added to the carboxyl terminus of the *Yersinia pseudotuberculosis* invasin protein interfere with recognition by integrin receptors. J. Biol. Chem. **268**:15840–15846.
31. **Kampik D, Schulte R, Autenrieth IB.** 2000. *Yersinia enterocolitica* invasin protein triggers differential production of interleukin-1, interleukin-8, monocyte chemoattractant protein 1, granulocyte-macrophage colony-stimulating factor, and tumor necrosis factor alpha in epithelial cells: implications for understanding the early cytokine network in *Yersinia* infections. Infect. Immun. **68**:2484–2492.
32. **Kirjavainen V, et al.** 2008. *Yersinia enterocolitica* serum resistance proteins YadA and Ail bind the complement regulator C4b-binding protein. PLoS Pathog. **4**:e1000140.
33. **Levy P, Robin H, Kornprobst M, Capeau J, Cherqui G.** 1998. Enterocytic differentiation of the human Caco-2 cell line correlates with alterations in integrin signaling. J. Cell Physiol. **177**:618–627.
34. **Losada L, et al.** 2011. Genome sequencing and analysis of *Yersina pestis* KIM D27, an avirulent strain exempt from select agent regulation. PLoS One **6**:e19054.
35. **Lutz R, Bujard H.** 1997. Independent and tight regulation of transcriptional units in *Escherichia coli* via the LacR/O, the TetR/O and AraC/I1-I2 regulatory elements. Nucleic Acids Res. **25**:1203–12310.
36. **Manoil C, Beckwith J.** 1986. A genetic approach to analyzing membrane protein topology. Science **233**:1403–1408.
37. **Marra A, Isberg RR.** 1996. Analysis of the role of invasin during *Yersinia pseudotuberculosis* infection of mice. Ann. N. Y. Acad. Sci. **797**:290–292.
38. **Marra A, Isberg RR.** 1996. Common entry mechanisms. Bacterial pathogenesis. Curr. Biol. **6**:1084–1086.
39. **Marra A, Isberg RR.** 1997. Invasin-dependent and invasin-independent pathways for translocation of *Yersinia pseudotuberculosis* across the Peyer's patch intestinal epithelium. Infect. Immun. **65**:3412–3421.
40. **McClelland M, et al.** 2001. Complete genome sequence of *Salmonella enterica* serovar Typhimurium LT2. Nature **413**:852–856.
41. **Meinzer U, et al.** 2008. Nod2 mediates susceptibility to *Yersinia pseudotuberculosis* in mice. PLoS One **3**:e2769.
42. **Monack DM, Mecsas J, Ghori N, Falkow S.** 1997. *Yersinia* signals macrophages to undergo apoptosis and YopJ is necessary for this cell death. Proc. Natl. Acad. Sci. U. S. A. **94**:10385–10390.
43. **Monk IR, Casey PG, Cronin M, Gahan CG, Hill C.** 2008. Development of multiple strain competitive index assays for *Listeria monocytogenes* using pIMC; a new site-specific integrative vector. BMC Microbiol. **8**:96.
44. **Nagel G, Lahrz A, Dersch P.** 2001. Environmental control of invasin expression in *Yersinia pseudotuberculosis* is mediated by regulation of

RovA, a transcriptional activator of the SlyA/Hor family. Mol. Microbiol. **41**:1249–1269.
45. **Nobbs AH, Lamont RJ, Jenkinson HF.** 2009. *Streptococcus* adherence and colonization. Microbiol. Mol. Biol. Rev. **73**:407–450.
46. **Nummelin H, et al.** 2004. The *Yersinia* adhesin YadA collagen-binding domain structure is a novel left-handed parallel beta-roll. EMBO J. **23**: 701–711.
47. **Oelschlaeger TA.** 2001. Adhesins as invasins. Int. J. Med. Microbiol. **291**: 7–14.
48. **Pepe JC, Miller VL.** 1993. The biological role of invasin during a *Yersinia enterocolitica* infection. Infect. Agents Dis. **2**:236–2341.
49. **Pepe JC, Wachtel MR, Wagar E, Miller VL.** 1995. Pathogenesis of defined invasion mutants of *Yersinia enterocolitica* in a BALB/c mouse model of infection. Infect. Immun. **63**:4837–4848.
50. **Remaut H, Waksman G.** 2004. Structural biology of bacterial pathogenesis. Curr. Opin. Struct. Biol. **14**:161–170.
51. **Saltman LH, Lu Y, Zaharias EM, Isberg RR.** 1996. A region of the *Yersinia pseudotuberculosis* invasin protein that contributes to high affinity binding to integrin receptors. J. Biol. Chem. **271**:23438–23444.
52. **Sambrook J, Russell DW.** 2001. Molecular cloning: a laboratory manual, 3rd ed. Cold Spring Harbor Laboratory Press, Cold Spring Harbor, NY.
53. **Schmid Y, et al.** 2004. Yersinia enterocolitica adhesin A induces production of interleukin-8 in epithelial cells. Infect. Immun. **72**:6780–6789.
54. **Schulze-Koops H, et al.** 1993. Outer membrane protein YadA of enteropathogenic yersiniae mediates specific binding to cellular but not plasma fibronectin. Infect. Immun. **61**:2513–2519.
55. **Sing A, Roggenkamp A, Geiger AM, Heesemann J.** 2002. *Yersinia enterocolitica* evasion of the host innate immune response by V antigen-induced IL-10 production of macrophages is abrogated in IL-10-deficient mice. J. Immunol. **168**:1315–1321.
56. **Steen A, et al.** 2005. AcmA of *Lactococcus lactis* is an N-acetylglucosaminidase with an optimal number of LysM domains for proper functioning. FEBS J. **272**: 2854–2868.
57. **Strong PC, et al.** 2011. Identification and characterisation of a novel adhesin Ifp in *Yersinia pseudotuberculosis.* BMC Microbiol. **11**:85.
58. **Thanassi DG.** 2011. The long and the short of bacterial adhesion regulation. J. Bacteriol. **193**:327–328.
59. **Toma C, et al.** 2004. Distribution of putative adhesins in different seropathotypes of Shiga toxin-producing *Escherichia coli.* J. Clin. Microbiol. **42**:4937–4946.
60. **Tsai JC, et al.** 2010. The bacterial intimins and invasins: a large and novel family of secreted proteins. PLoS One **5**:e14403.
61. **Uliczka F, Kornprobst T, Eitel J, Schneider D, Dersch P.** 2009. Cell invasion of *Yersinia pseudotuberculosis* by invasin and YadA requires protein kinase C, phospholipase C-gamma1 and Akt kinase. Cell Microbiol. **11**:1782–1801.
62. **Uliczka F, et al.** 2011. Monitoring of gene expression in bacteria during infections using an adaptable set of bioluminescent, fluorescent and colorigenic fusion vectors. PLoS One **6**:e20425.
63. **Viboud GI, Bliska JB.** 2005. Yersinia outer proteins: role in modulation of host cell signaling responses and pathogenesis. Annu. Rev. Microbiol. **59**: 69–89.
64. **Yang Y, Merriam JJ, Mueller JP, Isberg RR.** 1996. The *psa* locus is responsible for thermoinducible binding of *Yersinia pseudotuberculosis* to cultured cells. Infect. Immun. **64**:2483–2489.